4.2 RADIO EMISSION FROM SUPERNOVA REMNANTS*

D. K. MILNE
Division of Radiophysics, CSIRO, Sydney, Australia

Abstract. Observations of the radio emission from supernova remnants are reviewed with emphasis on the dissimilarity between the Crab Nebula and the other remnants. From this we conclude that there may be several non-thermal sources in the Galaxy with the same centrally filled structure as the Crab. These are, however, more evolved, and clearly there is no other source of the same age and type as the Crab Nebula.

1. Introduction

The identification of the radio source Taurus A, the Crab Nebula, with the supernova of 1054 AD, is undoubtedly correct. However, as many have remarked, Tau A bears little resemblance to the other discrete non-thermal galactic radio sources also generally supposed to be the remnants of supernovae. The extremely high radio brightness of Tau A leaves little chance that another object of this type (and evolutionary stage) remains undiscovered in the Galaxy, but there is still the possibility that among the known supernova remnants (SNRs) there exist old, well-evolved, objects of the Tau A type. In this paper we review the results that have been obtained from radio observations of SNRs with this possibility in mind.

2. Basic Observable Quantities: Flux Density, Spectrum, Size

There are now more than 100 SNRs known in the Galaxy. A catalogue listing over 90 of the brightest objects was published recently (Milne, 1970a) and a dozen additional objects of low brightness have since been found in 408 and 5000 MHz surveys (Shaver and Goss, 1970). A complete catalogue of these objects with their radio parameters, angular size, 1 GHz flux density, spectral index and surface brightness is given in Table I. This is a revised version of Milne's catalogue with the Shaver and Goss objects added. A discussion of the possible evolutionary effects shown by the sources in the original catalogue has been given by Milne (1970a) and the general conclusions are not altered by the revisions or the inclusion of the additional SNRs. A brief account of this work is given here.

Firstly, the spectral index of these objects has an average value of -0.48 ± 0.1. There does not appear to be any relationship between spectral index and surface brightness or diameter (contrary to Harris' (1962) findings). There appears to be a relationship between surface brightness, Σ, and linear diameter, D. This relationship, derived from 15 SNRs with known distances and for an average type SNR, is

$$\Sigma = 9.52 \times 10^{-15} D_{(PC)}^{-4.54} \text{ W m}^{-2} \text{ Hz}^{-1} \text{ sr}^{-1}, \quad (1)$$

with the further possibility that for type I SNRs the surface brightness is lower than

* This paper was presented by Dr. V. Radhakrishnan.

Davies and Smith (eds.), The Crab Nebula, 248–262.

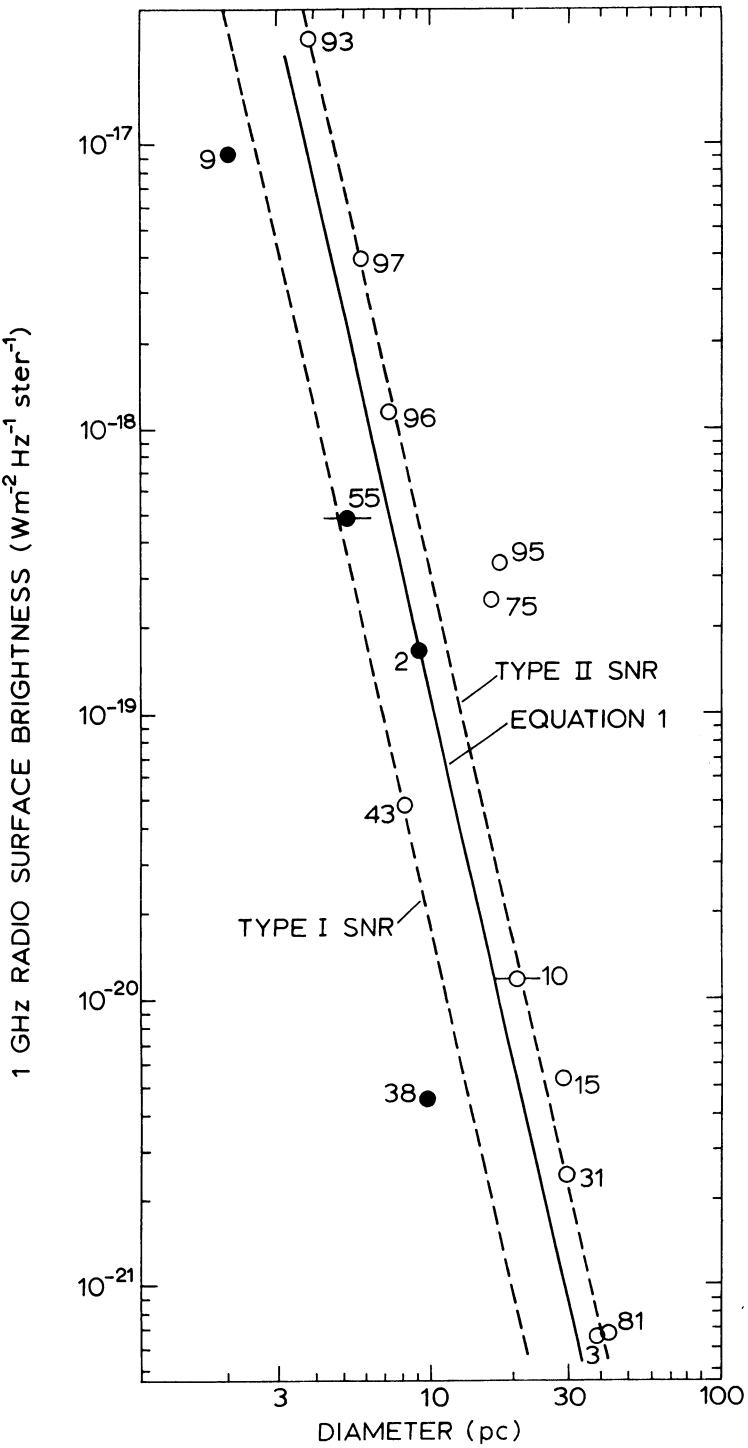

Fig. 1. The relationship between 1 GHz surface brightness and linear diameter for 15 SNRs whose distances are known. The filled circles represent those objects believed to be type I SNR. The numbers against each are the catalogue numbers of Table I. Possible evolutionary tracks for each type of SNR and the mean track (Equation (1)) are indicated in this figure.

https://doi.org/10.1017/S0074180900007531 Published online by Cambridge University Press

for the type II objects of the same diameter. This relationship is displayed in Figure 1. The decrease in surface brightness with increase in diameter and with SNR type (and hence initial energy) is consistent with Shklovsky's (1960) evolutionary theory, although the power of D in Equation (1) (-4.54) is not as high as was predicted by Shklovsky (-6.0). Kesteven (1968) points out that if the emitting region were a shell expanding at constant thickness then this value of -4.5 would be correct. This assumption of constant shell thickness is however contrary to the observations quoted in Section 3, and an alternative model satisfying Equation (1) should be sought. Van der Laan's (1962a, b) shell models, whilst accounting for the structure and polarization in SNRs, are not able to explain the high-surface-brightness objects (e.g. Cassiopeia A) or the evolutionary track in the Σ–D plane. It does seem that the observed evolution of the radio emission supports a degradation of the magnetic field and particle energy density (Shklovsky) rather than an intensification (van der Laan).

Using the average Σ–D relation (Equation (1)) Milne computed the linear diameters and distances of the SNRs and showed that the galactic distribution has certain features coincident with the HI spiral arms. This distribution, for the SNRs in Table I, is shown in Figure 2. The majority of SNRs are within ± 200 pc of the galactic plane with a half-density thickness of 80 pc, a population I distribution. The total SNR contribution to the galactic radio power (from 10 MHz to 10 GHz) is

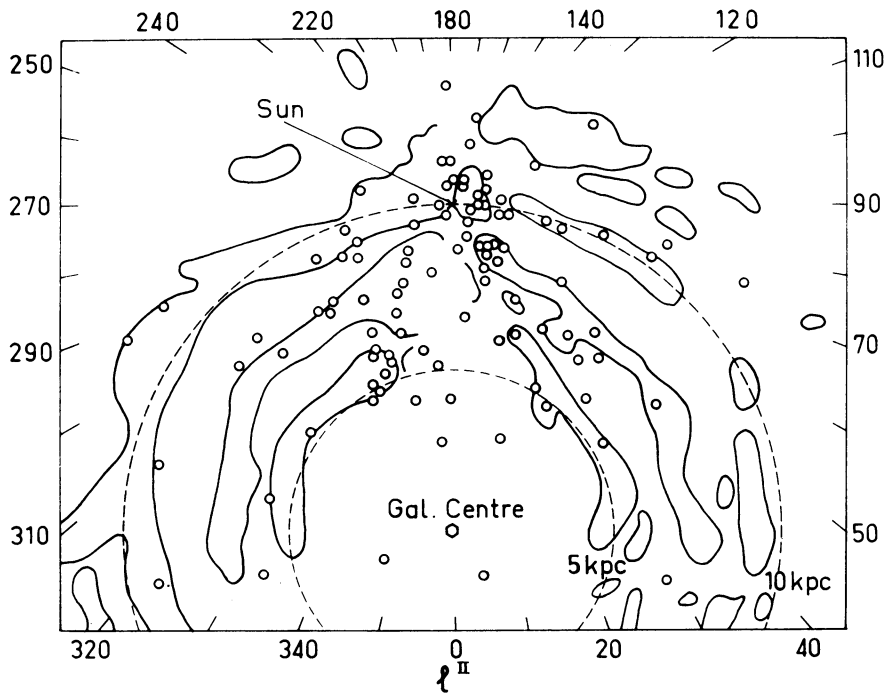

Fig. 2. Galactic distribution of SNRs derived from the distances in Table I. The outlined regions indicate the distribution of neutral hydrogen.

https://doi.org/10.1017/S0074180900007531 Published online by Cambridge University Press

TABLE I

Radio data for supernova remnants

(1) Catalogue No.	(2) Galactic source number	(3) Angular size $\phi_1 \times \phi_2$ (min arc)	(4) Flux density at 1 GHz S_0 (fu)[a]	(5) Spectral index at 1 GHz α	(6) Surface brightness at 1 GHz Σ unit[b]	(7) Diameter D (pc)	(8) Distance d (kpc)	(9) Ref.[c]	(10) Remarks
1	G119.5 + 10.0	125′ dia	38	−0.2	2.89E − 22	37.3	1.0		CTA 1
2	G120.1 + 1.4	6.0 × 7.0	58	−0.74	1.64E − 19	9.3	4.9	1	Tycho's Nova
3	G132.4 + 2.2	80′ dia	36	−0.7	6.70E − 22	31.1	1.4		HB 3
4	G156.4 − 1.2	300 × 120	225	−0.5	7.43E − 22	30.3	0.6		CTB 13
5	G160.5 + 2.8	120 × 140	150	−0.35	1.06E − 21	28.1	0.8		HB 9
6	G166.2 + 4.3	45′ dia	6.6	(−0.5)	3.88E − 22	35.0	2.7		VRO 42.05.01
7	G166.3 + 2.4	75′ dia	10.0	−0.5	2.12E − 22	40.0	1.9		OA 184
8	G180.0 − 1.7	180′ dia	120	−0.3?	4.41E − 22	34.0	0.7		S147
9	G184.6 − 5.8	3.0 × 4.2	1000	−0.25	9.45E − 18	3.8	1.7		Crab Neb., Tau A
10	G189.1 + 2.9	40′ dia	160	−0.45	1.19E − 20	16.5	1.4		IC 443
11	G193.3 − 1.5	80′ dia	27	−0.5	5.03E − 22	33.1	1.4		0607 + 17
12	G205.5 + 0.2	210′ dia	150	−0.5	4.05E − 22	34.7	0.6		Monoceros Neb.
13	G260.4 − 3.4	55′ dia	145	−0.5	5.70E − 21	19.4	1.2		Puppis A
14	G261.9 + 5.5	35′ dia	10.0	−0.38	9.70E − 22	28.6	2.9		0902 − 38
15	G263.4 − 3.0	220 × 180	1800	−0.30	5.40E − 21	19.6	0.4		Vela X, Y and Z
16	G284.2 − 1.8	23 × 12	25	−0.46	1.05E − 20	16.9	3.5		MSH 10 − *53*
17	G289.1 − 0.4	3.0 × 3.2	20	−0.65	2.48E − 19	8.5	9.4		
19	G290.1 − 0.8	13 × 12	80	−0.5	6.10E − 20	11.5	3.2	2	MSH 11 − *61A*
20	G291.0 − 0.1	10′ dia	25	−0.57	2.97E − 20	13.5	4.6	2	MSH 11 − *62*
21	G292.0 + 1.8	2.8 × 2.7	15	−0.36	2.37E − 19	8.5	10.8		MSH 11 − *54*
22	G295.1 − 0.6	13 × 14	29	−0.6	1.87E − 20	14.9	3.8		Kes 16
23	G296.3 + 10.0	86 × 75	49	−0.52	9.05E − 22	29.1	1.3		1209 − 51/52
23a	G298.5 − 0.2	27′ dia	10	−0.33	1.63E − 21	25.5	3.3	2	
24	G304.6 + 0.1	5.2 × 6.1	15	−0.50	5.62E − 20	11.7	7.2		Kes 17
26	G307.6 − 0.3	3′.7 dia	24	−0.45	2.09E − 19	8.8	8.2		
27	G309.6 + 1.7	6′.3 dia	47	−0.60	1.41E − 19	9.6	5.3		13S6A B
28	G309.7 + 1.8	7.1 × 5.4	83	−0.60	2.58E − 19	8.4	4.7	(3.6)[d]	13S6A A

https://doi.org/10.1017/S0074180900007531 Published online by Cambridge University Press

Table 1 (continued)

(1) Catalogue No.	(2) Galactic source number	(3) Angular size $\phi_1 \times \phi_2$ (min arc)	(4) Flux density at 1 GHz S_0 (fu)[a]	(5) Spectral index at 1 GHz α	(6) Surface brightness at 1 GHz Σ unit[b]	(7) Diameter D (pc)	(8) Distance d (kpc)	(9) Ref.[c]	(10) Remarks
29	G310.6 − 0.3	7′.5 dia	9	−0.6	1.91E − 20	14.9	6.9		Kes 20B } (3.3)[d]
30	G310.8 − 0.4	8 × 11	20	−0.35	2.71E − 20	13.8	5.1		Kes 20A }
30a	G311.5 − 0.3	3′.9 dia	3.7	−0.49	2.89D − 20	13.6	12.0	2	
31	G315.4 − 2.3	40′ dia	33	−0.5	2.46E − 21	23.3	2.0		MSH 14 − 63
32	G316.3 + 0.0	13′ dia	24.3	−0.47	1.71E − 10	15.2	4.0	2	MSH 14 − 57
33	G320.4 − 1.2	26′ dia	58.4	−0.53	1.03E − 20	17.0	2.3	2	MSH 15 − 52
35	G322.3 − 1.2	2′.6. dia	4.2	−0.7	7.56E − 20	11.0	14.6		Kes 24
36	G326.2 − 1.7	11 × 8.6	145	−0.24	1.84E − 19	9.0	3.2		MSH 15 − 56
37	G327.4 + 0.4	10′ dia	26	−0.78	3.10E − 20	13.4	4.6		Kes 27
38	G327.6 + 14.5	30 × 22	25	−0.63	4.52E − 21	20.4	2.8		1459 − 41
38a	G328.0 + 0.3	5′.9 dia	2.4	−0.55	8.20E − 21	17.9	10.5	2	
39	G328.4 + 0.2	4′.2 dia	17.5	−0.5	1.18E − 19	10.0	8.2	2	MSH 15 − 57
40	G330.0 + 15.0	270′ dia	340	−0.3	5.56E − 22	32.4	0.4		Lupus Loop
41	G332.0 + 0.1	12′.0 dia	9.1	−0.48	7.52E − 21	18.2	5.2	2	
42	G332.5 + 0.1	15′ dia	26	−0.47	1.39E − 20	15.9	3.7	2	MSH 16 − 51
43	G332.4 − 0.4	9′ dia	24	−0.43	3.53E − 20	13.0	5.0	2	1613 − 50
43a	G333.0 + 0.3	2′.6 dia	8.3	−0.17	1.46E − 19	9.5	12.6	2	
44	G336.7 + 0.5	11′ dia	6.3	−0.49	6.20E − 21	19.0	6.0	2	
45	G337.0 − 0.1	14′ dia	17	−0.5	1.04E − 20	17.0	4.2	2	Part of CTB 33
46	G337.3 + 1.0	11′ dia	15	−0.2	1.48E − 20	15.7	5.0		Kes 40
47	G337.8 − 0.1	6′.5 dia	17.7	−0.5	4.99E − 20	12.0	6.4	2	Kes 41
47a	G338.1 + 0.4	12′.0 dia	4.5	−0.42	3.72E − 21	21.3	6.1	2	
47b	G338.3 − 0.0	8′.9 dia	15.1	−0.65	2.27E − 20	14.3	5.5	2	
47c	G338.5 + 0.1	8′.2 dia	28.3	−0.30	5.01E − 20	12.0	5.1	2	
48	G342.1 + 0.1	30′ dia	54	−0.5	7.15E − 21	18.4	2.1		MSH 16 − 48
49	G348.5 + 0.1	8.1 × 5.3	84	−0.5	2.33E − 19	18.6	4.5		CTB 37 A } (2.4)[d]
50	G348.7 + 0.3	3.8 × 6.0	47	−0.5	2.44E − 19	8.5	6.1		CTB 37 B }
51	G349.7 + 0.2	1.9 × 2.6	23	−0.6	5.54E − 19	7.1	11.0		

https://doi.org/10.1017/S0074180900007531 Published online by Cambridge University Press

Table 1 (continued)

(1) Catalogue No.	(2) Galactic source number	(3) Angular size $\phi_1 \times \phi_2$ (min arc)	(4) Flux density at 1 GHz S_0 (fu)[a]	(5) Spectral index at 1 GHz α	(6) Surface brightness at 1 GHz Σ unit[b]	(7) Diameter D (pc)	(8) Distance d (kpc)	(9) Ref.[a]	(10) Remarks
52	G355.3 + 0.1	7.5 × 9.5	30	−0.6	5.01E − 20	12.0	4.9		NGC 6383
53	G357.7 − 0.1	4.4 × 3.4	38	−0.6	3.02E − 19	8.1	7.2		MSH 17 − *39*
54	G359.4 − 0.1	5.7 × 6.7	29	−0.4	9.05E − 20	10.6	5.9		
55	G4.5 + 6.8	2′.2 dia	20.0	−0.58	4.92E − 19	7.3	11.4		Kepler's Nova
56	G.53 − 1.1	12 × 18	38	−0.3	2.06E − 20	14.6	3.4		A4
57	G6.5 − 0.1	45′ dia	300	−0.40	3.97E − 20	15.1	1.3	4	A1, W28
58	G11.2 − 0.4	4′.6 dia	22	−0.52	1.27E − 19	9.8	7.3	2	
59	G18.9 + 0.3	7.0 × 14	35	−0.57	4.25E − 10	12.5	4.4		MSM 18 − *18*
60	G21.8 − 0.5	20′ dia	69	−0.52	2.05E − 20	14.6	2.5	2	MSH 18 − *113*
61	G23.1 + 0.0	45 × 60	350	−0.22	1.54E − 20	15.6	1.0		W41
61a	G23.6 + 0.3	9′.8 dia	7.6	−0.34	9.42E − 21	17.4	6.1	2	
61b	G24.5 + 0.2	7′.2 dia	10.0	−0.22	2.30E − 20	14.3	6.8	2	
61c	G24.7 + 0.6	14′.0 dia	13.4	−0.38	8.14E − 21	17.9	4.4	2	
62	G27.3 + 0.0	32′ dia	41	−0.4	4.77E − 21	20.2	2.2		
63	G29.7 − 0.2	2′.1 dia	11.1	−0.6	3.08E − 19	8.1	13.2	2	4C − 03.70
64	G31.9 + 0.0	3′.5 dia	22	−0.50	2.13E − 19	8.7	8.6		3C 391
65	G32.0 − 4.9	60′ dia	19	−0.45	6.28E − 22	31.5	1.8		3C 396.1
66	G33.0 + 0.1	31 × 10	25	−0.4?	9.16E − 21	17.3	3.4		
67	G33.7 + 0.0	7.3 × 5.6	12	−0.5	3.49E − 20	13.0	7.1		4C + 00.7
68	G34.6 − 0.5	28 × 35	230	−0.40	2.79E − 20	13.7	1.5		W44
69	G35.6 − 0.4	10′ dia	25	−0.3	2.98E − 20	13.5	4.7		
70	G37.6 − 0.1	30′ dia	48	−0.6	6.35E − 21	18.9	2.2		W47
71	G39.2 − 0.3	6′.7 dia	21	−0.44	5.54E − 20	11.8	6.1	2	NRAO 593
72	G39.7 − 2.0	50′ dia	48	−0.7	2.29E − 21	23.7	1.6		W50
73	G41.1 − 0.3	10′ × 8′	17	−0.3	2.53E − 20	14.0	5.3		3C 397
74	G41.9 − 4.1	165 × 140	150	−0.5?	7.74E − 21	30.0	0.7		CTB 72
75	G43.3 − 0.2	4′.8 dia	38.7	−0.47	2.00E − 19	8.9	6.4	2	W49B
76	G45.5 + 0.1	3.9 × 2.9	23	−0.4	2.42E − 19	8.5	8.7	2	Kuzmin 47

https://doi.org/10.1017/S0074180900007531 Published online by Cambridge University Press

Table 1 (continued)

(1) Catalogue No.	(2) Galactic source number	(3) Angular size $\phi_1 \times \phi_2$ (min arc)	(4) Flux density at 1 GHz S_0 (fu)[a]	(5) Spectral index at 1 GHz α	(6) Surface brightness at 1 GHz Σ unit[b]	(7) Diameter D (pc)	(8) Distance d (kpc)	(9) Ref.[c]	(10) Remarks
77	G46.8 − 0.3	12′ × 5′	18	−0.5	3.57E − 20	12.9	5.8		
78	G47.6 + 6.1	60′ dia	12	(−0.5)	3.97E − 22	34.8	20		CTB 63
79	G49.2 − 0 5	26′ dia	160	−0.25	2 82E − 20	13.6	1.8	1	Part of W51
80	G53.7 − 2.2	20′ dia	8.5	−0.6	2.53E − 21	23.2	4.0		3C 400.2
81	G74.0 − 8.6	200 × 160	180	−0.45	6.70E − 22	31.1	0.6		Cygnus Loop
82	G74.8 + 0.6	4.7 × 3.9	(10)	(−0.15)	6.50E − 20	11.4	9.2		
83	G74.9 + 1.2	9.3 × 4.7	(18)	(−0.5)	4.89E − 20	12.1	6.3		
84	G78.1 + 1.8	30 × 20	230	−0.7	4.56E − 20	12.3	1.7		W66, CTB 91
85	G78.3 + 2.5	13.3 × 9.5	18	−0.2	1.71E − 20	15.3	4.7		DR 3
86	G78.5 − 0.1	9.5 × 8.0	8	−0.2	1.25E − 20	16.3	6.5		DR 12
87	G78.6 + 1.0	12 × 15	54	−0.5	3.57E − 20	12.9	3.4		
88	G78.9 + 3.7	37 × 38	180	−0.2	1.52E − 20	15.6	1.4		DR 1
89	G79.8 + 1.2	13 × 29	39	−0.2	1.23E − 20	16.4	2.9		DR 11
90	G82.2 + 5.4	100 × 60	160	−0.25	2.66E − 21	22.3	1.0	3	W63
91	G89.1 + 4.7	105′ dia	225	−0.35	2.43E − 21	23.5	0.8	5	HB 21
92	G93.6 − 0.3	54′ dia	45	−0.69	1.83E − 21	24.9	1.6		CTB 104
93	G111.7 − 2.1	4.0 × 3.8	3000	−0.72	2.34E − 17	3.1	2.7		Cas A
94	G117.3 + 0.1	130′ dia	55	−0.5	3.87E − 21	35.1	0.9		CTB 1
95	L.M.C.	1′.12 dia	3.5	−1.01	3.33E − 19	7.9	24.5		N49 S } 3SNRs in
96	L.M.C.	0′.45 dia	1.9	−0.50	1.12E − 18	6.1	46.5		N63 A } the
97	L.M.C.	0′.37 dia	4.6	−0.50	4.00E − 18	4.6	42.8		N132 E } L.M.C.

[a] 1 fu = 10^{-26} W m^{-2} Hz^{-1}

[b] W m^{-2} Hz^{-1} sr^{-1}

[c] References are: 1 Dickel (1969), 2 Shaver and Goss (1970), 3 Wendker (1968), 4 Milne and Wilson (1971), 5 Erkes and Dickel (1969)

[d] Possibly components of the one source, at the distances shown in parentheses.

https://doi.org/10.1017/S0074180900007531 Published online by Cambridge University Press

5.5×10^{36} erg sec^{-1}, or about $\frac{1}{100}$ of the total radio emission from the Galaxy. The cumulative size distribution obtained for these objects, $D \propto [N(D' < D)]^{2/5} \propto t^{2/5}$ (where $N(D' < D)$ is the number of SNRs with diameters D' less than some given diameter D and t is the age of a SNR with diameter D), suggests that SNRs follow Sedov's (1959) treatment for an adiabatic explosion in a gas of constant heat capacity,

$$D_{(\mathrm{PC})} = 4.0 \times 10^{-11} (E_0/n_H)^{1/5} t_{(\mathrm{yr})}^{2/5}, \tag{2}$$

where E_0 (erg) is the initial energy of the explosion and n_H (cm^{-3}) is the ambient hydrogen number density in the medium.

3. Structural Characteristics of Supernova Remnants

Of approximately 55 objects listed in Table I for which observations of sufficient resolution have been made, 30 show a peripheral distribution of radio brightness indicating a shell structure, 6 show possible shell structure, a further 6 have a crescent structure which could indicate a rudimentary shell, and there are 3 well-resolved double sources. Thus a total of 45 SNRs exhibit a peripheral brightness distribution. There are possibly 9 objects which, although sufficiently well-resolved, do not appear to have any structure in their brightness distributions. The Crab Nebula is the brightest of these objects and has been observed with the highest resolution.

In Figure 3 we show characteristic contours (generally $\frac{1}{4}$, $\frac{1}{2}$ and $\frac{3}{4}$ power isotherms) of 43 of the resolved SNRs. The peripheral brightness distribution interpreted as shell structure can be seen in at least 36 of these. In this figure the SNR diagrams have been arranged in descending order of surface brightness and therefore, according to Figure 1, in order of increasing linear dimensions. The diagrams are (with the exception of SNR 93, Cas A) all drawn to the same linear scale corresponding to the distance given in Table I. The galactic plane is horizontal in these diagrams. There is nothing of an evolutionary nature immediately obvious in the structure of these objects nor does there seem to be any preferred orientation relative to the galactic plane. On this first point Shaver and Goss (1970) found for 19 well-resolved shells with diameters 3 to 40 pc that the relative shell thickness is fairly constant at near 15% of the diameter. However, these estimates are subjective and rather uncertain with the individual thickness/diameter ratios varying from 8% to 25%. It does seem though that the relative shell thickness is reasonably constant throughout Figure 3 and certainly they do not evolve at the constant shell thickness required by Kesteven (1968) in his interpretation of the Σ–D relationship (Figure 1, Equation (1)).

Another point raised by Shaver's work from 18 sources is that the brightest regions of a SNR lie each side of a diameter parallel to the galactic plane (Shaver, 1969). This result does not appear to be borne out in the examples shown in Figure 3. There are 30 SNRs in Figure 3 for which an axis of symmetry can be defined; the average angle made by these axes and the galactic plane is 45°. Nor does the situation improve much if we delete those SNRs which are more than 50 pc from the galactic plane; the average angle then is 52°, a slight but inconclusive shift towards Shaver's result.

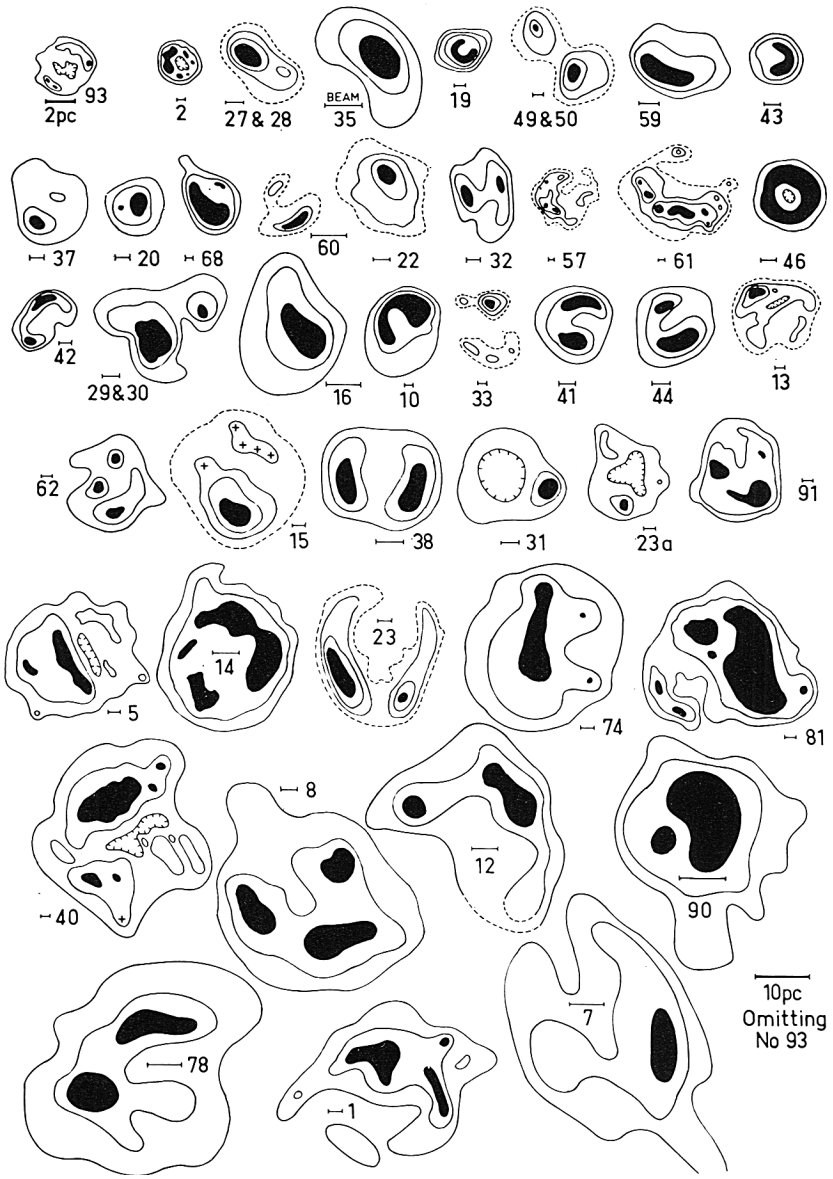

Fig. 3. The structural characteristics of 43 well-resolved SNRs. The contour levels shown are quarter-power, half-power and three-quarter power (shaded): in a few cases one-eighth power contours are shown (broken lines) and for SNR 19 the 90% contour level is shown shaded to indicate the shell. With the exception of SNR 93 (Cas A) the isotherms are all drawn to the same linear scale corresponding to the distances given in Table I. The diagrams are arranged in order of surface brightness. The galactic plane is horizontal in each case. The observing beamwidth is indicated on each diagram.

https://doi.org/10.1017/S0074180900007531 Published online by Cambridge University Press

Detailed analyses of the radial distribution of SNR brightness (e.g. Hill, 1967; Baldwin, 1967; Kesteven, 1968; Wynn-Williams, 1969; Rosenberg, 1970) show that for several SNRs the central part of the source is not as bright as expected from a uniform and isotropically emitting shell model fitted to the outer rim emission. Rosenberg has offered an explanation (for Cas A) in terms of a preferred direction of the synchrotron emission from the shell, this being due to a partial radial alignment of the magnetic field.

Lastly, one might expect that objects well off the galactic plane, where density variations of interstellar gas are less severe, would show the most uniform structure. However, in Figure 3, where $|z|$ ranges up to 700 pc, no obvious differences in structure are apparent. It is still possible that the expansion rate is greater for those objects away from the plane, but this should not affect their structural appearance, nor the Σ–D relationship.

4. Polarized Radio Emission from Supernova Remnants

Using a resolution sufficient to clearly resolve the shell structure, linearly polarized radio emission of the order of a few per cent is observed from most of the brighter SNRs. Seventeen SNRs are known to be polarized and detailed polarization maps at several frequencies have been constructed for at least 14 of these objects. The main feature is the low degree of polarization usually found, showing magnetic field disorder. In only a few cases is the degree high enough to suggest a simple model. A radial magnetic field is suggested for three of these sources: Cas A (Mayer and Hollinger, 1968), 1459−41 (SN 1006 AD) (Kundu, 1970) and IC 443 (Milne, 1971), although in this latter source there is a possibility that the magnetic field, initially parallel to the galactic plane, has been blown out by the expansion in the transverse directions (see Figure 4b). In other SNRs the magnetic field is directed predominantly along the shell (a tangential field). Examples of this are found in 1209−51/52 (Whiteoak and Gardner, 1968), W44 (Kundu and Velusamy, 1969), Vela X (Milne, 1968a) and W28 (Milne and Wilson, 1971 and Kundu, 1970).

With a particular source, in mind (1209−51/52) Whiteoak and Gardner (1968) interpret these two predominating field directions in terms of van der Laan's models, the radial magnetic fields being observed when the line of sight is along the ambient magnetic field and the tangential field when viewed transversely to the magnetic field. The SNRs in which the field is radial should show circular symmetry in their radio structure (a more complete shell) whilst tangential fields should be observed in SNRs exhibiting, ideally, a double crescent brightness distribution. There does not seem to be a great deal of verification of these principles in the examples we have. The situation is, however, not generally as simple as Whiteoak and Gardner suggest; local irregularities are common, and in many SNRs there are regions where the field is radial alongside other regions where a tangential field is suggested (e.g. W28 (Milne and Wilson, 1971), Puppis A and MSH 14−63 (Milne – unpublished data)).

It is only in those SNRs where a fairly uniformly directed field extends across the

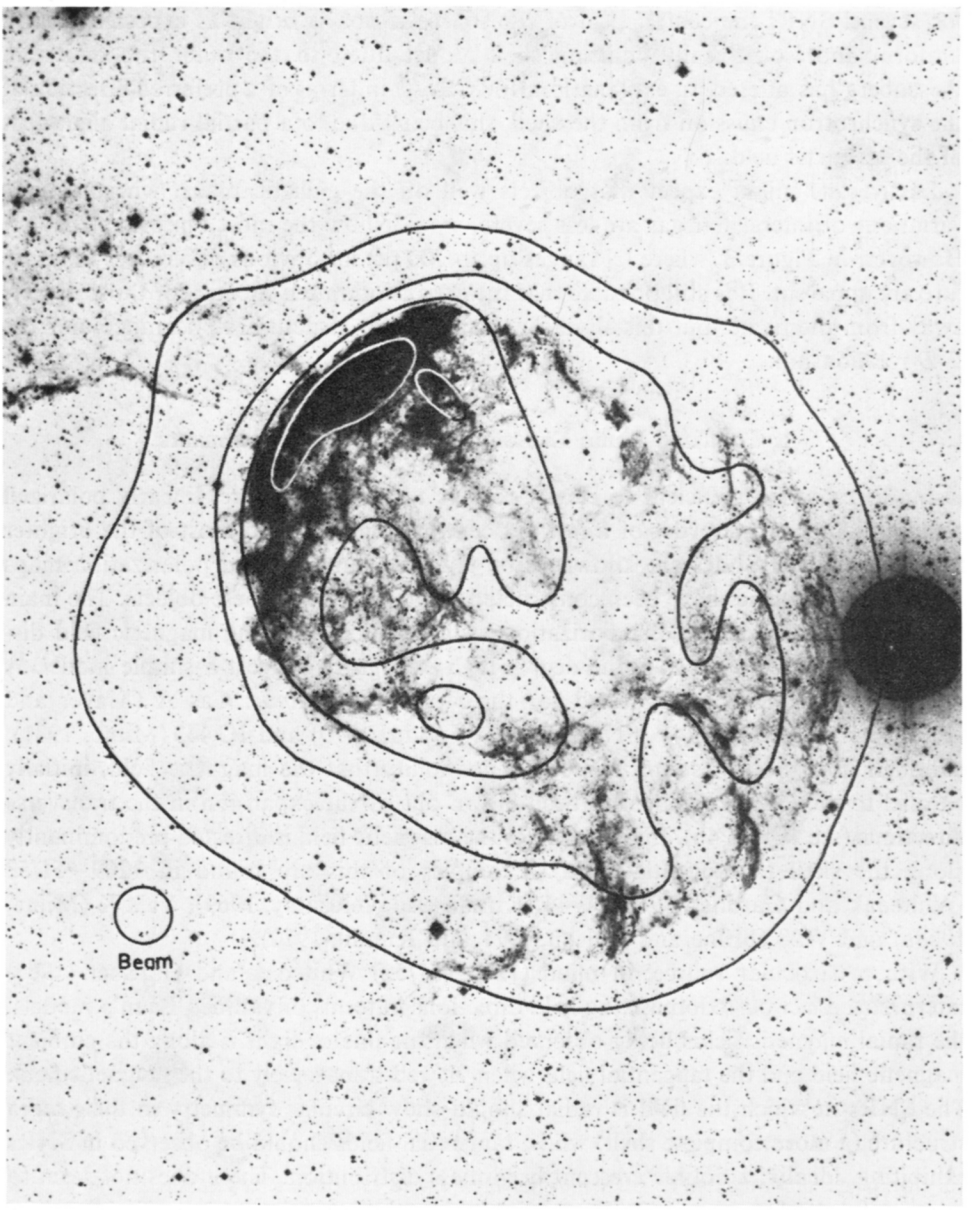

Fig. 4a. 5000 MHz isotherms superimposed on a red 48′ Schmidt photograph of IC 443 (Milne, 1971). The shell structure in this supernova remnant is well defined at both radio and optical wavelengths; the good radio-optical agreement shown here is the exception rather than the rule amongst SNRs.

https://doi.org/10.1017/S0074180900007531 Published online by Cambridge University Press

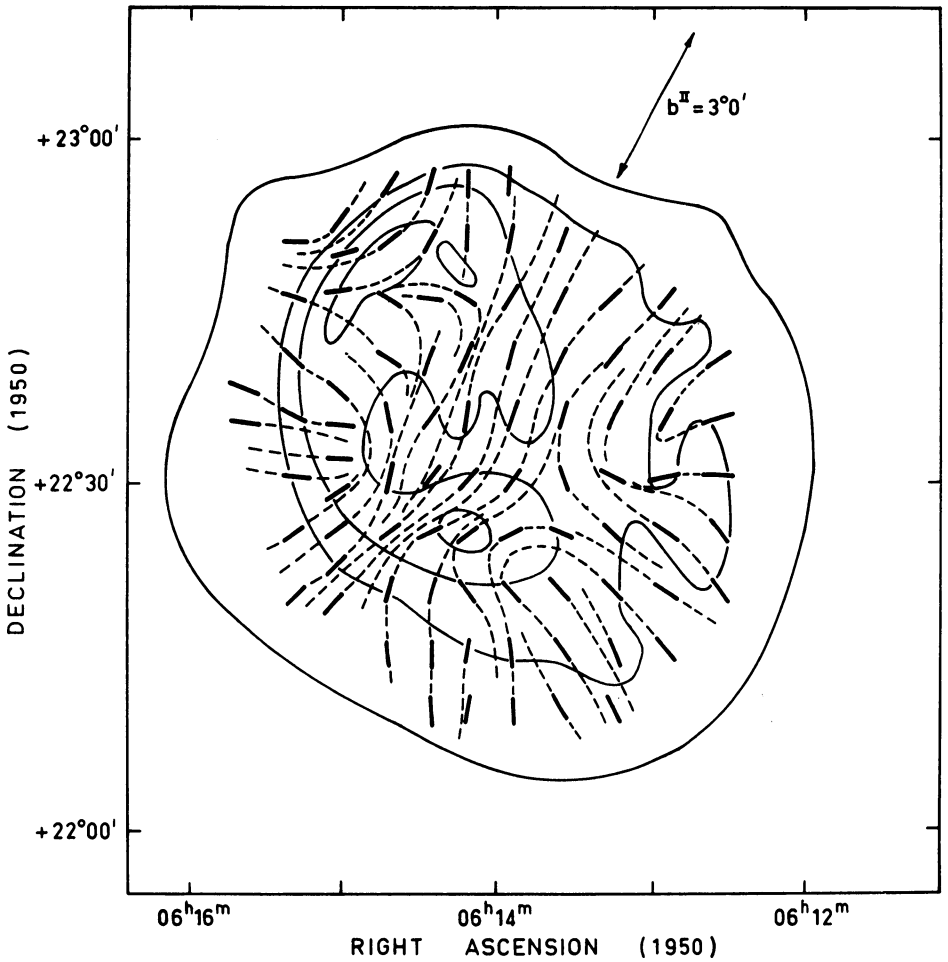

Fig. 4b. The projected directions of magnetic field in IC 443; the contours are those of Figure 4a. The magnetic field is predominantly radial (Milne, 1971).

source, or where the polarization is from a small region, that polarization is detectable at low resolutions; examples of this are W44 and Tau A. One object which exhibits relatively high polarization and has no shell structure is MSH 15−*56* (SNR No. 36), which consists of an 11′ × 9′ central core imbedded in a halo 30′ diam. (Milne, 1969); this SNR has polarization up to 10% at 6 cm (Gardner *et al.*, 1969). It has a high surface brightness and has been suggested as a possible X-ray source (Poveda and Woltjer, 1968; Milne, 1970b).

5. Optically Identified Supernova Remnants

There are seventeen galactic SNRs well identified with visible nebulae. Most of these can only be seen as a few faint, often sharp, filamentary wisps (e.g. Cas A, Pup A

https://doi.org/10.1017/S0074180900007531 Published online by Cambridge University Press

and Kepler's Nova). In a few cases they are moderately bright and clearly exhibit a shell structure (e.g. IC 443, S 147, the Cygnus Loop and Vela X). In most cases the agreement between radio and optical brightness distribution is very poor in detail but as a general rule one can say that the optical filaments outline the region containing the radio emission. It has been demonstrated that these filaments are 'sheets seen edge on', possibly the best argument for this model being the observations of temperature gradation within the filaments – difficult to justify physically with a circular filament model (Parker, 1964, 1969; Milne, 1968b).

One exception to the rule of poor detailed radio-optical agreement is in IC 443 (Figure 4a), where the brightest radio emission coincides with the optical shell. Milne (1971) finds that the spectral index is flatter (more thermal) around this shell and most likely is a blend of thermal and nonthermal components. An appreciable free-free radio contribution in IC 443 is in fact deduced by this author from the Hα intensity; contrary to an earlier calculation (Hogg, 1964), this would explain the detailed radio-optical agreement.

6. The Association of Supernova Remnants with Pulsars and X-Ray Sources

The discovery of a pulsar in the Crab Nebula (Staelin and Reifenstein, 1969) and in Vela X (Large *et al.*, 1968) led to searches in other well-known SNRs but without success. There is no acceptable positional agreement between the 41 pulsars listed by Radhakrishnan (1969) and Large *et al.* (1969) and the SNRs in Table I except for the two already noted. Large (1970) has in fact predicted that pulsars would be undetectable in all but the closest SNRs, with the present limitations on sensitivity and dispersion.

A similar comparison with the X-ray sources has yielded far better but possibly fortuitous results because of the large probable errors in the X-ray positions. Milne (1970b) lists seven SNRs within the error circles for the X-ray sources. Of these three have been identified with SNRs: Tycho's Nova, the Crab Nebula and Cas A. Of special interest is the SNR close to Nor X−2, MSH 15−*56* (SNR 36), already singled out in this review; this source has, like the Crab, high surface brightness (hence comparatively young), fairly flat spectral index, high polarization and an absence of radio structure. The other possibly significant suggested identification is that of GX5−1 with A4 (SNR 56). The source GX5−1 has a well-established position (1·2′ error radius) and lies within SNR 56; it is suggested here that this is a definite identification.

7. Conclusions

Summarizing the radio observations we find that:

(1) There is an average evolutionary relationship

$$\Sigma = 9.52 \times 10^{-15} D^{-4.54}, \tag{1}$$

with variations from this probably dependent on the initial energy. There is no noticeable evolutionary effect on the spectral index.

(2) The expansion probably follows Sedov's equation

$$D = 4.0 \times 10^{-11} (E_0/n_H)^{1/5} t^{2/5} . \quad (2)$$

(3) Almost all of the resolved SNRs exhibit some form of peripheral brightness distribution indicating possible shell structure. The relative shell thickness is fairly constant.

(4) There seems to be no preferred galactic orientation and no latitude effects in the structure.

(5) Radio polarization of the order of a few per cent has been found in many SNRs, but generally the direction of polarization varies so much across the source that polarization is not observed until the shell is well resolved. The magnetic field distribution is mostly tangential; however, in many objects there are regions with tangential field adjacent to other regions in which the field is clearly radial.

(6) There is generally no detailed radio-optical brightness correlation. The source IC 443, one of the few objects that show a strong agreement, has a large thermal component.

(7) There are two known SNR-pulsar associations and possibly 7 SNRs which emit X-radiation.

Briefly summarizing the properties of the Crab Nebula in relation to the other SNRs, we have:

(1) It has a high surface brightness and its position (No. 9) on the Σ–D diagram (Figure 1) is well off to the low initial energy side of the average evolutionary track. It is still possible that it is an average type I SNR, if such a classification exists. From Equation (2) we obtain an initial energy/ambient hydrogen density ratio (E_0/n_H) of 10^{48} erg cm^3, considerably lower than any of the other SNRs with known ages.

(2) Taurus A has a spectral index of -0.25, flatter than most SNRs and possibly flatter than all of the SNRs with well-determined spectral indices.

(3) Even at high resolution Tau A exhibits a relatively amorphous brightness distribution (Hogg *et al.*, 1969). In this respect it is unlike almost all of the other resolved SNRs. We have however pointed out that there may be eight other SNRs with no apparent structure and these may well form a Tau A type class.

(4) At low resolutions the percentage radio polarization from Tau A is greater than is found in most other unresolved SNRs, and the high resolution observations of Mayer and Hollinger (1968) show that the magnetic field is uniformly directed over most of the source.

(5) The Crab Nebula contains both a pulsar and a source of X-rays.

In conclusion, are there any other Tau A type objects within the Galaxy? Certainly there are no other known Tau A type objects at the same stage of evolution. Possibly MSH 15−*56* (SNR 36) is a later stage in the evolution of these objects, and it is further possible that the flat spectrum SNRs 11−*54* (SNR 21) and A4 (SNR 56) are also well-evolved members of this class. High-resolution searches locating more amorphous non-thermal galactic sources should yield the answer to this question.

References

Baldwin, J. E.: 1967, *IAU Symp.* **31**, 337.
Dickel, J. R.: 1969, *Astrophys. Letters* **4**, 109.
Erkes, J. W. and Dickel, J. R.: 1959, *Astron. J.* **74**, 840.
Gardner, F. F., Whiteoak, J. B., and Morris, D.: 1969, *Australian J. Phys.* **22**, 821.
Harris, D. E.: 1962, *Astrophys. J.* **135**, 661.
Hill, E. R.: 1967, *Australian J. Phys.* **20**, 297.
Hogg, D. E.: 1964, *Astrophys. J.* **140**, 992.
Hogg, D. E., MacDonald, G. H., Conway, R. G., and Wade, C. M.: 1969, *Astron. J.* **74**, 1206.
Kesteven, M. J.: 1968, *Australian J. Phys.* **21**, 739.
Kundu, M. R.: 1970, *Astrophys. J.* **162**, 17.
Kundu, M. R. and Velusamy, T.: 1969, *Astrophys. J.* **155**, 807.
Large, M. I.: 1970, *Astrophys. Letters* **5**, 11.
Large, M. I., Vaughan, A. E., and Mills, B. Y.: 1968, *Nature* **220**, 340.
Large, M. I., Vaughan, A. E., and Wielebinski, R.: 1969, *Nature* **223**, 1249.
Mayer, G. H. and Hollinger, J. P.: 1968, *Astrophys. J.* **151**, 53.
Milne, D. K.: 1968a, *Australian J. Phys.* **21**, 201.
Milne, D. K.: 1968b, *Australian J. Phys.* **21**, 501.
Milne, D. K.: 1969, *Australian J. Phys.* **22**, 613.
Milne, D. K.: 1970a, *Australian J. Phys.* **23**, 425.
Milne, D. K.: 1970b, *Proc. Astron. Soc. Austr.* **1**, 333.
Milne, D. K.: 1971, 'Radio Observations of the Supernova Remnants IC 443 and Puppis A', *Australian J. Phys.* (in press).
Milne, D. K. and Wilson, T. L.: 1971, *Astron. Astrophys.* **10**, 220.
Parker, R. A. R.: 1964, *Astrophys. J.* **139**, 493.
Parker, R. A. R.: 1969, *Astrophys. J.* **155**, 359.
Poveda, A. and Woltjer, L.: 1968, *Astron. J.* **73**, 65.
Radhakrishnan, V.: 1969, *Proc. Astron. Soc. Austr.* **1**, 254.
Rosenberg, I.: 1970, *Monthly Notices Roy. Astron. Soc.* **147**, 215.
Sedov, L. I.: 1969, *Similarity and Dimensional Methods in Mechanics*, Academic Press, New York.
Shaver, P. A.: 1969, Cornell-Sydney University Astronomy Centre, Preprint No. 137.
Shaver, P. A. and Goss, W. M.: 1970, *Australian J. Phys. Astrophys.*, Suppl. No. 14.
Shklovsky, I. S.: 1960, *Soviet Astron.* **4**, 243.
Staelin, D. H. and Reifenstein, E. C.: 1969, *Astrophys. J.* **156**, L121.
van der Laan, H.: 1962a, *Monthly Notices Roy. Astron. Soc.* **124**, 125.
van der Laan, H.: 1962b, *Monthly Notices Roy. Astron. Soc.* **124**, 179.
Wendker, H.: 1968, *Z. Astrophys.* **69**, 392.
Whiteoak, J. B. and Gardner, F. F.: 1968, *Astrophys. J.* **154**, 807.
Wynn,Williams, C. G.: 1969, *Monthly Notices Roy. Astron. Soc.* **142**, 453.

Discussion

L. Woltjer: How does one know that all these objects are really supernova remnants?

V. Radhakrishnan: One concludes that they must be from their spectrum, size, etc. There is no absolute proof as far as I know.